

Thermal characterization of near-infrared laser quantum-well GaSb-based sources

V. K. Kononenko^a, E. P. Sachkov^a, V. M. Stetsik^a, P. Christol^b

^a Stepanov Institute of Physics NASB, 220072 Minsk, Belarus

e-mail: lavik@dragon.bas-net.by

^b IES-Université Montpellier 2, CNRS 5214, 34095 Montpellier, France

Thermal properties and energy parameters are determined for quantum-well heterostructure lasers in the GaInAsSb–AlGaAsSb system, which emit at the wavelengths of 2.1–2.4 μm . It is shown that the characteristic temperature of the threshold current is about of 76 K. Role of the Auger recombination is discussed and a method of determining the activation energy for such a process is approved.

Keywords: quantum well, laser, characteristic temperature, Auger recombination, activation energy.

Introduction

Quantum-well (QW) heterostructure lasers and light-emitting diodes are widely applied in the photonic industry and particularly in spectroscopy and metrology. To assure required semiconductor source lifetime, efficiency, power, and emission spectrum, the diode junction temperature must be precisely controlled.

Laser diodes of near- and mid-IR diapasons are needed for purposes of tunable diode laser spectroscopy (TDLS) for high-sensitive gas analysis and environmental monitoring [1, 2]. Particular, the most of pollutant molecule gases (CO₂, CO, NH₃, CH₄, HF, *etc.*) have absorption lines in the 2–3 μm wavelength range. In this range, GaSb-based laser diodes are more preferable and applied [3–6]. The laser diodes are also attractive as a source in distance-type pyrometer sensors for control of heated metal temperature.

Results presented in the work are concerned with a characterization of QW heterostructure lasers in the GaInAsSb–AlGaAsSb system, which emit at the wavelengths of 2.1–2.4 μm . From lasing threshold measurements versus temperature of the active region, the characteristic temperature of the threshold is determined. Role of Auger recombination (AR) processes is analyzed and a method of determining the activation energy for definite channels is approved. Thermal properties of the laser diodes are obtained from data of transient characteristics under self-heating by direct current.

1. Temperature sensitivity of the laser threshold

At the operation temperature growth, the threshold of the long-wavelength lasers increases mainly because of AR rate enhancement [7]. Weakening the temperature sensitivity of the threshold can be realized in asymmetric multiple-QW heterostructures (AMQWHs) [8]. Lasers with AMQWH in the active region are attractive for multi-channel optical network and TDLS technique.

Generally, the threshold current density in QW heterostructure lasers j_{th} is determined by the threshold quantity of the two-dimensional spontaneous radiative recombination rate R_{sp} in the active region, *i. e.*, $j_{\text{th}} = eR_{\text{sp}} / \eta' \eta_{\text{sp}}$. Here, η' is the injection efficiency and η_{sp} is the quantum yield of spontaneous emission, which characterizes the role of useless recombination processes in the active region, including ones through different defects and non-radiative AR.

At direct dipole optical transitions, the threshold j_{th} changes linearly versus the temperature T where losses in the cavity are not very high. The violation of the electron wave vector conservation [9] and involving the high-lying subbands at the transitions result in increasing the power of the dependence $j_{\text{th}}(T)$ and functionally $j_{\text{th}} \sim T^n$, where n in the range of

1 to 3. In practice, the temperature dependence of the threshold is described by an exponential function with the characteristic parameter T_0 . According to the determining of T_0 one has at a narrow operation temperature interval $T \approx T_{\text{op}}$ roughly $T_0 \approx T_{\text{op}}/n$.

To distinguish the AR rate, we present the threshold in the form $j_{\text{th}} = e(A n_{\text{th}}^n + C n_{\text{th}}^3)/\eta'$, where n_{th} is the threshold sheet concentration of electrons. The coefficient A is determined by the optical transition probability and for the direct transitions ($n = 1$) it can be taken as $A \approx 1/\tau_{\text{sp}}$, where τ_{sp} is the threshold lifetime of current carriers [10]. As a rule, the AR coefficient c is determined in the activation approach, *i.e.*, $c \approx c_0 \exp(-E_{\text{act}}/kT)$ [7, 11]. The activation energy is related to the energy of transitions between corresponding subband levels E_q as $E_{\text{act}} \approx E_q \delta_m$, where δ_m is the effective-mass relation. Generally, procedure of the determining of C in QW heterostructures, especially for strained laser systems, is rather complex [12, 13].

If $n_{\text{th}} \sim T$, we obtain for the characteristic parameter T_0 a definition [14, 15]

$$T_0 \approx \frac{T_{\text{op}}}{n + (1 - \eta_{\text{sp}})(3 - n + E_{\text{act}}/kT_{\text{op}})}. \quad (1)$$

As seen, where the role of the AR becomes essential ($\eta_{\text{sp}} \ll 1$), the value of the parameter T_0 is determined by the ratio of the activation energy E_{act} and thermal energy kT_{op} . On the other hand, from the measurements of T_0 it is possible to evaluate the effective value of the activation energy of the AR processes.

2. Experimental

The laser structures were defined for growth on the GaSb substrate. The active region of the GaInAsSb–AlGaAsSb heterolasers consist of three QWs (10 nm width) and waveguide region (0.8 μm width). Basic heterostructure includes an undoped $\text{Al}_{0.35}\text{Ga}_{0.65}\text{As}_{0.03}\text{Sb}_{0.97}$ waveguide layer that is sandwiched between $\text{Al}_{0.90}\text{Ga}_{0.10}\text{As}_{0.08}\text{Sb}_{0.92}$ cladding layers ensuring optical confinement. These quaternary alloys are lattice matched to the substrate. A thin highly doped *p*-type GaSb cap layer is placed for the making of an ohmic contact.

In quasi-strained structure, the active region contains three QWs of the $\text{Ga}_{0.6}\text{In}_{0.4}\text{As}_{0.1}\text{Sb}_{0.9}$ compound. In this case, the band offsets in the conduction and valence bands are equal to $\Delta E_c = 0.597$ eV and $\Delta E_v = 0.135$ eV. For the $\text{Al}_{0.35}\text{Ga}_{0.65}\text{As}_{0.03}\text{Sb}_{0.97}$ barrier layers we have the energy gap $E_g = 1.167$ eV, Luttinger parameters $\gamma_1 = 10.48$ and $\gamma_2 = 3.46$, effective masses $m_{\text{cb}} = 0.075m_0$, $m_{\text{vhb}} = 0.281m_0$, and $m_{\text{vlb}} = 0.057m_0$. The $\text{Ga}_{0.6}\text{In}_{0.4}\text{As}_{0.1}\text{Sb}_{0.9}$ QWs characterizes ($T = 300$ K) by $E_g = 0.435$ eV, $\gamma_1 = 20.98$, $\gamma_2 = 8.58$, $m_c = 0.031m_0$, $m_{\text{vh}} = 0.262m_0$, $m_{\text{vl}} = 0.026m_0$, $m_{\text{vht}} = 0.034m_0$, $m_{\text{vlt}} = 0.081m_0$, $m_s = 0.12m_0$, and $\Delta_s = 0.738$ eV. The compound parameters are obtained by interpolation of the data of binary and/or ternary compounds.

Active QW layers are grown in plane (100). Therefore the longitudinal components of the effective masses of heavy and light holes, which determine the energy levels of the valence subbands, are found as $m_{\text{vh}} = m_e / (\gamma_1 - 2\gamma_2)$ and $m_{\text{vl}} = m_e / (\gamma_1 + 2\gamma_2)$, respectively, and the transverse components, which determine the density of states, are equal to $m_{\text{vht}} = m_e / (\gamma_1 + \gamma_2)$ and $m_{\text{vlt}} = m_e / (\gamma_1 - \gamma_2)$.

The obtained laser diodes having narrow stripe contact (5 μm) emit in CW operation regime at wavelengths near $\lambda_{\text{st}} = 2.12$ μm and $\lambda_{\text{st}} = 2.35$ μm at room temperature. Lasers with wide stripe contact (100 μm) operate in pulsed regime and emit stimulated multi-mode emission at wavelengths near $\lambda_{\text{st}} = 2.38$ μm .

Analysis of transient measurements gives values of the thermal resistance R_T of the

GaInAsSb–AlGaAsSb heterolasers in the range of 50 to 140 K/W [16]. Mention that more important and informative parameter is the specific value of thermal resistance (per unit square), which lies in the range 8–20 mm² K/W. Dominant including in R_T is related to the heat time constant τ_T of 1–6 ms and corresponds to attachment of laser chips to copper plates and the quality of the laser source package has especially to be improved.

It should be noted that obtained GaSb-based laser diodes have enough large series resistances (specific resistance is of $7 \times 10^{-4} \Omega \text{ cm}^2$) as follows from direct current–voltage characteristics. In particular, optical power efficiency versus pump current for the long-wavelength laser ($\lambda_{\text{st}} = 2.35 \mu\text{m}$) above the threshold ($\approx 25 \text{ mA}$) demonstrates low efficiency (< 10 %) that can be attributed to a great Joule heat at diode series resistance (which is up to 14 Ω). If the heat losses at the series resistance are excluded from electrical power, a possible high efficiency quantity (up to 37 %) can be obtained that is close to values for ordinary near-IR QW heterolasers [16].

Temperature dependence of the threshold current density $j_{\text{th}}(T)$ for the GaInAsSb–AlGaAsSb laser emitting at $\lambda_{\text{st}} = 2.38 \mu\text{m}$ is shown in Fig. 1. The laser sample has 100 μm -wide stripe contact and pulsed threshold current is of 220 mA at room temperature. In the operation temperature interval 250–320 K, the dependence $j_{\text{th}}(T)$ follows an exponential function with the characteristic temperature approximately of $T_0 = 76 \text{ K}$. Such a value is conditioned, obviously, due to enough high rate of useless AR processes in the active region.

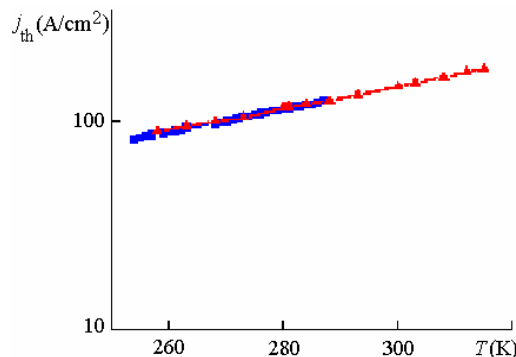


Fig. 1. Dependence of the threshold current density $j_{\text{th}}(T)$ for the GaInAsSb laser.

3. Auger recombination coefficient

Calculations of the AR rate in the laser active region are made according to the conventional method [7, 11]. The most important carrier interactions are considered, *i. e.*, CHCC, CHLH, and CHSH types. Processes of CHSH and/or CLLS types with states of the split-off valence band are not essential because of a large value of the split-off separation energy Δ_s in the investigated GaSb-based lasers. The coefficient C_0 for considered AR processes can be written approximately as $C_0 = 4e^4 |V_T|^2 \alpha / \hbar k T \varepsilon^2$, where ε is the dielectric constant of the crystal, V_T is the matrix element of the carrier interactions at the threshold energy for a definite AR process to take place. The factor α for each from channels CHCC, CHHH, and CHLH is determined by corresponding ratio of the effective masses of carriers involving in the processes [14].

The activation energy E_{act} of AR is related to the energy of transitions between corresponding subband levels E_q and can be given in the following expressions for each processes, *e. g.*, CHCC and CHLH, respectively,

$$E_{\text{act}}^{\text{CHCC}} = \frac{\mu_h}{1 + \mu_h} E_h, \quad E_{\text{act}}^{\text{CHLH}} = \frac{\mu_h}{\mu_l \mu_h + 2\mu_l - \mu_h} (E_h - \Delta_{lh}), \quad (2)$$

where $\Delta_{lh} = E_l - E_h$, E_h and E_l are the transition energies between electron and heavy and light hole states. We assume that applied expressions in the Boltzmann approximation [7, 11] can be also used for evaluations at degeneracy in the subbands. Ratios μ_h and μ_l are equal, respectively, to $\mu_h = m_c/m_{vht}$ and $\mu_l = m_c/m_{vlt}$. Here, m_c is the effective mass of electrons, m_{vit} is the transverse component of the effective mass of heavy or light holes ($i = h$ or l).

For the $\text{Ga}_{0.6}\text{In}_{0.4}\text{As}_{0.1}\text{Sb}_{0.9}\text{--Al}_{0.35}\text{Ga}_{0.65}\text{As}_{0.03}\text{Sb}_{0.97}$ QW heterostructure we obtain $E_h = 0.50$ eV, $E_l = 0.53$ eV, $\Delta_{lh} = 0.03$ eV, $\mu_h = 0.91$, $\mu_l = 0.38$. Then, corresponding parameters α and δ_m are equal to $\alpha^{\text{CHCC}} = 0.22$, $\alpha^{\text{CHLH}} = 0.27$, $\delta_m^{\text{CHCC}} = 0.48$, and $\delta_m^{\text{CHLH}} = 4.5$. Therefore, the activation energy E_{act} of AR processes occurs to be of 0.2 eV. The most essential is the process of CHCC type. The activation energy for transitions of CHLH type is rather high (2.1 eV). So, the CHCC process is the most important channel of AR with the energy activation of the order of 0.2 eV.

Detail calculations show that concentration of current carriers (electron and holes) in the active region at inversion and lasing conditions reaches up to $3.6 \times 10^{11} \text{ cm}^{-2}$. In this case, the rate of spontaneous recombination is about of $R_{\text{sp}} = 9 \times 10^{20} \text{ cm}^{-2} \text{ s}^{-1}$. If the activation energy of AR processes is of 0.2 eV, it is possible from Eq. (1) to evaluate the quantum yield of spontaneous emission η_{sp} . We found $\eta_{\text{sp}} \approx 0.8$. It gives the quantity of non-radiative recombination rate $Q \approx 2.2 \times 10^{20} \text{ cm}^{-2} \text{ s}^{-1}$. Then we can to determine the value of AR coefficient, *i. e.*, $C = 4.8 \times 10^{-15} \text{ cm}^4 \text{ s}^{-1}$. Obviously, the volume value of AR coefficient C_v is related with the surface (sheet) AR coefficient C as $C_v = Cd^2$, where d is the QW width ($d = 10 \text{ nm}$). Therefore, one has to obtain $C_v = 4.8 \times 10^{-27} \text{ cm}^6 \text{ s}^{-1}$. Such a value is similar to quantities known in Refs. [1, 2, 17].

For investigated GaSb-based laser structures we can also found the value of C_0 . At conditions of $T = 300 \text{ K}$ and $E_{\text{act}} = 0.2 \text{ eV}$, we obtain AR parameter $C_0 = 1.1 \times 10^{-11} \text{ cm}^4 \text{ s}^{-1}$. Therefore the CHCC process is the most important channel of AR recombination with the energy activation of the order of 0.2 eV and sheet coefficient C_0 of $1.1 \times 10^{-11} \text{ cm}^4 \text{ s}^{-1}$.

4. Discussion

The reverse task to determine the effective value of the activation energy of the AR processes in the active region or the quantum yield of spontaneous emission η_{sp} from the measurements of T_0 is also attractive. As an example, we use data for the GaInAsSb–GaSb type-II QW ridge-lasers emitting at $2.38 \mu\text{m}$ [18]. At the pulsed operation temperature $T_{\text{op}} = 300 \text{ K}$, measurements give the following characteristic temperature $T_0 = 60 \text{ K}$.

The energy E_q equals approximately $h\nu = 0.52 \text{ eV}$. Considering that more powerful non-radiative AR process is of CHCC type, we evaluate $\delta_m \approx \mu_h/(1+\mu_h)$, where $\mu_h = m_c/m_{vht}$. Since the electron QW corresponds to $\text{Ga}_{0.65}\text{In}_{0.35}\text{As}_{0.15}\text{Sb}_{0.85}$ and hole QW to GaSb, one can assume (from the binary component iteration) $m_c \approx 0.033m_e$ and $m_{vht} \approx 0.055m_e$. In this case, $\mu_h \approx 0.60$ and the following value for δ_m occurs to be $\delta_m \approx 0.38$ (*i. e.*, $E_{\text{act}} \approx 0.2 \text{ eV}$). Therewith, the parameter α equals $\alpha \approx 0.20$. Similar values occur for lasers emitting near $1.5 \mu\text{m}$ and for the more powerful non-radiative AR process of CHCC type [15].

According to Eq. (1), since $n \approx 2$, we obtain at room temperature $\eta_{\text{sp}} \approx 0.6$. This quantity η_{sp} is above than the internal quantum yield of stimulated emission $\eta_{\text{st}} = 0.45$ [18] and demonstrates enough high efficiency of optical transitions in staggered type-II QW heterostructure lasers.

In a bulk laser system, for GaSb–AlGaAsSb double-heterostructures ($\lambda_{\text{st}} = 1.77 \mu\text{m}$) [19], we found again that more powerful non-radiative AR process is of CHCC type with the activation energy of $E_{\text{act}} \approx 0.1 \text{ eV}$. Therewith, δ_m occurs to be $\delta_m \approx 0.14$ and $\alpha \approx 0.10$. As an experimental value $T_0 = 80 \text{ K}$ and the threshold carrier concentration in the active region is

about of $1.1 \times 10^{18} \text{ cm}^{-3}$ at room operation temperature, one evaluates at $\eta_{\text{sp}} \approx 0.67$ (if $n = 1$) or at $\eta_{\text{sp}} \approx 0.86$ (if $n = 2$) the volume AR coefficient $C_v \approx 0.3 \times 10^{-27} \text{ cm}^6 \text{ s}^{-1}$. As seen, it is also in close accordance with Refs. [1, 2, 17].

Obtained temperature change of the quantum yield of spontaneous emission $\eta_{\text{sp}}(T)$ at different values n according to Eq. (1) for the GaInAsSb–AlGaAsSb laser with $E_{\text{act}} = 0.2 \text{ eV}$ and $T_0 = 76 \text{ K}$ is presented in Fig. 3. Comparison of theoretical calculations in the model with no the \mathbf{k} -selection rule and measured threshold (Fig. 4) show good agreement at $n = 2$.

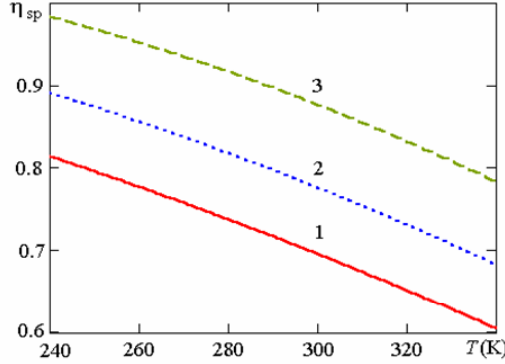


Fig. 2. Temperature change of $\eta_{\text{sp}}(T)$ at different values n (figures at the curves) for the GaInAsSb–AlGaAsSb laser with $E_{\text{act}} = 0.2 \text{ eV}$ and $T_0 = 76 \text{ K}$.

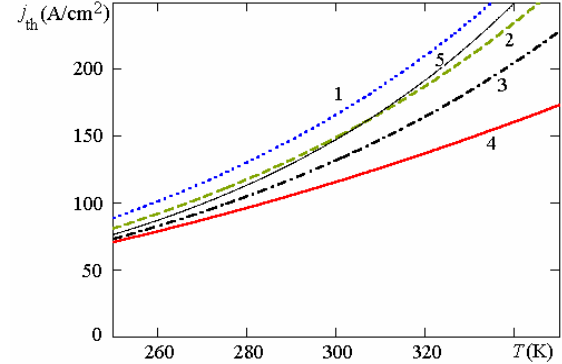


Fig. 3. Dependence $j_{\text{th}}(T)$ including $\eta_{\text{sp}}(T)$ at values $n = 1, 2, 3$ (figures at the curves) in comparison with calculated inversion current density (curve 4) and measured j_{th} (curve 5).

So, for the GaSb-based QW heterostructures under consideration, the CHCC processes introduce the main contribution to the total AR rate at the threshold. Such a behavior is associated with a lower specific E_{act} that is caused with smaller value of δ_m , as compared, *e. g.*, CHLH type process. For the GaSb-based lasers the effective energy E_{act} is of the order of 0.20 eV. The quantity of the coefficient C (and/or C_0) it is required to examine more precisely due to questions appeared in connection with the energy gap of different semiconductors [17] and a possibility of disorder on AR lifetimes, in particular, due to completely neglecting momentum conservation in AR transitions [20].

Conclusions

For the $\text{Ga}_{0.6}\text{In}_{0.4}\text{As}_{0.1}\text{Sb}_{0.9}\text{--Al}_{0.35}\text{Ga}_{0.65}\text{As}_{0.03}\text{Sb}_{0.97}$ QW heterostructure lasers the measured characteristic temperature of the threshold is about of 76 K. Role of AR is discussed and a method of determining the activation energy for non-radiative processes or the quantum yield of spontaneous emission is approved. As shown, the CHCC process is the most important channel of AR with the energy activation of the order of 0.2 eV. Thermal characterization of the diode sources is developed on investigation of transient processes under self-heating by direct current. It is shown that the dominant contribution to the internal thermal resistance of the laser diode sources is connected with a die attach layer.

In conclusion, the authors wish to thank A. Joullié, Ya. A. Bumai, and O. S. Vas'kov for their help and fruitful discussions.

References

1. Joullié A., Christol P. GaSb-based mid-infrared 2–5 μm laser diodes. *C. R. Physique*. 2003. Vol. 4, No. 6. P. 621–637.
2. Joullié A., Christol P., Baranov A. N., Vicet A. Mid-infrared 2–5 μm heterojunction laser diodes. *Topic Appl. Phys.* 2003. Vol. 80. P. 1–59.

3. Vicet A., Yarekha D. A., Pérona A., Rouillard Y., Gaillard S., Baranov A. N. Trace gas detection with antimonide-based quantum-well diode lasers. *Spectrochimica Acta, Part A: Mol. & Biomol. Spectrosc.* 2002. Vol. 58, No. 11. P. 2405–2412.
4. Geerlings E., Rattunde M., Schmitz J., Kaufel G., Zappe H., Wagner J. Widely tunable GaSb-based external cavity diode laser emitting around $2.3\text{ }\mu\text{m}$. *IEEE Photon. Technol. Lett.* 2006. Vol. 18, No. 18. P. 1913–1915.
5. Barat D., Angellier J., Vicet A., Rouillard Y., Le Gratiet L., Guilet S., Martinez A., Ramdane A. Antimonide-based lasers and DFB laser diodes in the $2\text{--}2.7\text{ }\mu\text{m}$ wavelength range for absorption spectroscopy. *Appl. Phys. B.* 2008. Vol. 90, No. 2. P. 201–204.
6. Civiš S., Cihelka J., Matulková I. Infrared diode laser spectroscopy. *Opto-Electron. Rev.* 2010. Vol. 18, No. 4. P. 408–420.
7. Agrawal G. P., Dutta N. K. *Long-Wavelength Semiconductor Lasers*. N. Y., 1986.
8. Kononenko V. K., Afonenko A. A., Manak I. S., Nalivko S. V. Asymmetric multiple quantum well heterostructure laser systems: conception, performance, and characteristics. *Opto-Electron. Rev.* 2000. Vol. 8, No. 3. P. 241–250.
9. Afonenko A. A., Manak I. S., Shevtsov V. A., Kononenko V. K. Radiative recombination rate in quantum-well structures in the model without \mathbf{k} -selection. *Semiconductors*. 1997. Vol. 31, No. 9. P. 929–932.
10. Kononenko V. K., Tsvirko V. I. Lifetime of current carriers at spontaneous radiative recombination in quantum wells. *Bull. RAS, Ser. Phys.* 2003. Vol. 67, No. 2. P. 223–226.
11. Sugimura A. Auger recombination effect on threshold current of InGaAsP quantum well lasers. *IEEE J. Quantum Electron.* 1983 Vol. QE-19, No. 6. P. 932–941.
12. Andreev A. D., Zegrya G. G. Auger recombination in strained quantum wells. *Semiconductors*. 1997. Vol. 31, No. 3. P. 297–303.
13. Andreev A. D., O'Reilly E. P. Theoretical study of Auger recombination in a GaInNAs $1.3\text{ }\mu\text{m}$ quantum well laser structure. *Appl. Phys. Lett.* 2004. Vol. 84, No. 11. P. 1826–1828.
14. Kononenko V. K., Ushakov D. V., Sukhoivanov I. A., Mashoshina O. V. Control of influence of Auger recombination on the threshold in asymmetric quantum-well lasers. *Proc. LFN M 2004*. Kharkiv, 2004. P. 107–111.
15. Sukhoivanov I. A., Mashoshyna O. V., Kononenko V. K., Ushakov D. V. How to restrain Auger recombination predominance in the threshold of asymmetric bi-quantum-well lasers. *Microelectron. J.* 2005. Vol. 36, No. 3. P. 264–268.
16. Bumai Yu. A., Vaskou A. S., Kononenko V. K. Measurement and analysis of thermal parameters and efficiency of laser heterostructures and light-emitting diodes. *Metrology and Measurement Systems*. 2010. Vol. 17, No. 1. P. 39–46.
17. Bulashevich K. A., Karpov S. Yu. Is Auger recombination responsible for the efficiency rollover in III-nitride light-emitting diodes? *Phys. stat. sol. (c)*. 2008. Vol. 5, No. 6. P. 2066–2069.
18. Joullié A., Glastre G., Blondeau R., Nicolas J. C., Cuminal Y., Baranov A. N., Wilk A., Garcia M., Grech P., Alibert C. Continuous-wave operation of GaInAsSb–GaSb type-II quantum-well ridge-lasers. *IEEE J. Select. Topic Quantum Electron.* 1999. Vol. 5, No. 3. P. 711–714.
19. Dolginov L. M., Drakin A. E., Druzhinina L. V., Eliseev P. G., Milvidskii M. G., Sverdlov B. N., Skripkin V. A. Injection lasers based on AlGaAsSb/GaSb and InGaAsSb/GaSb heterostructures. *Proc. PhIAN*. 1983. Vol. 141. P. 46–61.
20. Grein C. H., Ehrenreich H. J. Modeling of disorder influenced Auger recombination in strained-layer type-II superlattices. *Appl. Phys.* 2002. Vol. 93, No. 2. P. 1075–1078.